Supplementary Information

Supplementary Figures

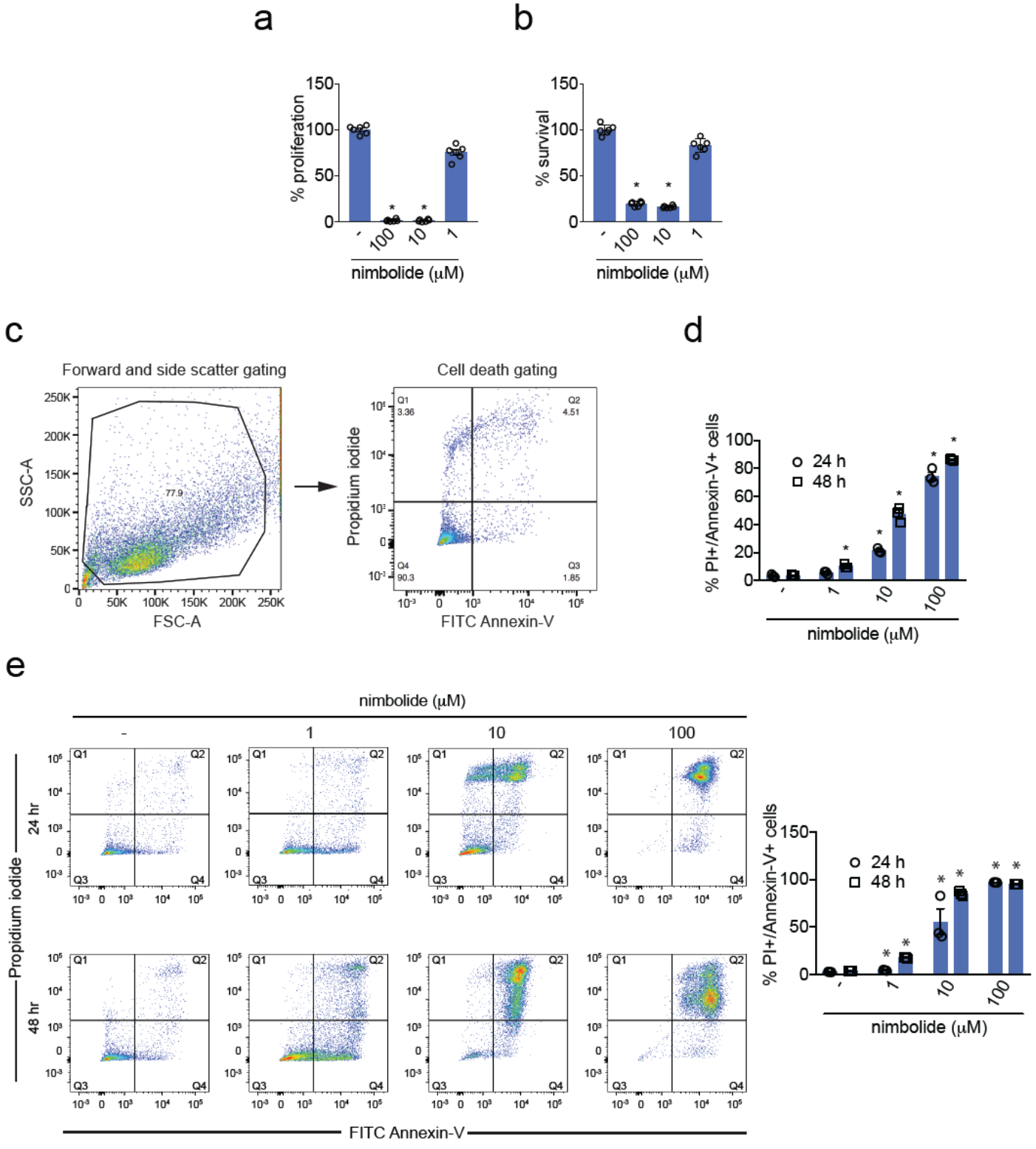

Supplementary Figure 1. Nimbolide impairs breast cancer cell proliferation and survival and induces apoptosis. (a, b) HCC38 breast cancer cell proliferation in serum-containing media **(a)** and serum-free cell survival **(b)**. Cells were treated with DMSO vehicle or nimbolide and cell viability was assessed after 48 h. **(c)** Shown is the gating strategy for the flow cytometry data. We used two gating steps--the first step we gated by forward and side scatter. The second gate was based on separation into quadrants by cell death stains (PI / annexin). **(d, e)** Percent of propidium iodide and Annexin-V-positive (PI+/Annexin-V+) cells assessed by flow

cytometry after treating 231MFP **(d)** and HCC38 **(e)** cells with DMSO vehicle or nimbolide for 24 or 48 h. Representative FACS data from 231MFP cells in **(d)** in shown in **Fig. 1d** and from HCC38 cells are shown in **(e)** on the left panels. Bar graphs in **(d, e)** are percentage of late-stage apoptotic cells defined as defined as PI+/Annexin-V+ cells. Data shown in **(a**, **b, d, e)** are average ± sem, n=6 in **(a, b)** and n=3 in **(d, e)** biologically independent samples/group. Statistical significance was calculated with unpaired two-tailed Student's t-tests. Significance is expressed as *p=1.64×10^{-13} and 2.05×10^{-13} for 100 and 10 μM, respectively for **(a)** and *p=2.09×10^{-11} and 7.07×10^{-12} for 100 and 10 μM, respectively for **(b)**, *p=9.05×10^{-5} and 1.87×10^{-5} for 10 and 100 μM, respectively for 24 h data for **(d)**, *p=0.00139, 0.000142, and 7.97×10^{-9} for 1, 10 and 100 μM, respectively for 48 h data for **(e),** *p=0.00424, 0.0182, and 2.22×10^{-11} for 1, 10 and 100 μM, respectively for 24 h data for **(e),** and *p=6.68×10^{-6}, 4.70×10^{-7}, and 9.00×10^{-11} for 1, 10 and 100 μM, respectively for 48 h data for **(e),** compared to vehicle-treated controls.

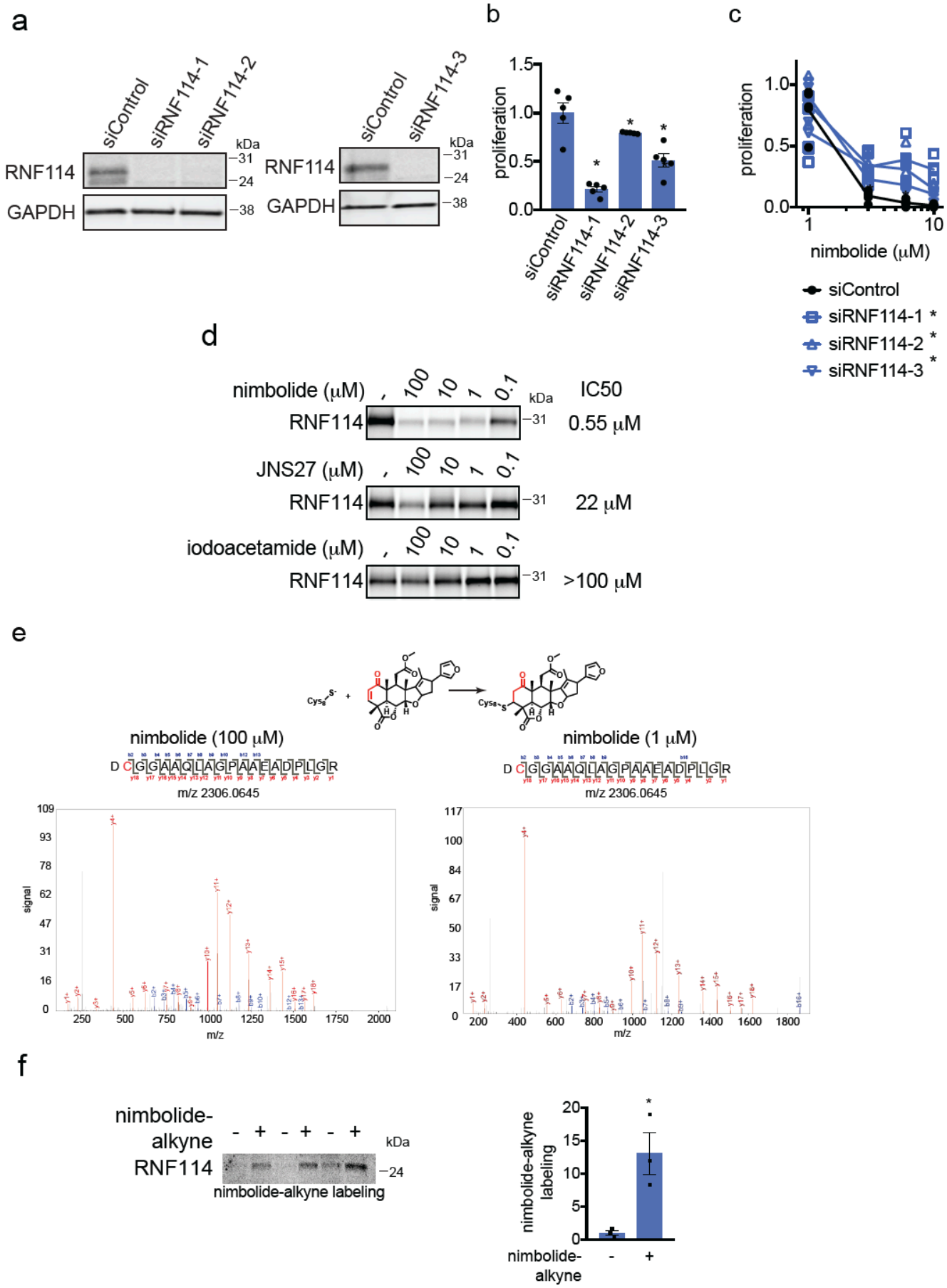

Supplementary Figure 2. Elucidating the Role of RNF114 in nimbolide-mediated effects. (a) RNF114 knockdown by 3 independent siRNAs targeting RNF114 validated by Western blotting of RNF114 compared to

siControl 231MFP cells. GAPDH expression is shown as a loading control. Full length and replicate blots are shown in **Supplementary Fig. 7a. (b)** 231MFP cell proliferation after 24 h in siControl and siRNF114 cells assessed by Hoechst stain. **(c)** Nimbolide effects on 231MFP siControl and siRNF114 231MFP breast cancer cells. Cells were treated with DMSO vehicle or nimbolide for 24 h after which proliferation was assessed by Hoechst stain. Data for each siControl or siRNF114 group was normalized to the respective DMSO vehicle control in each group. Individual biologically independent sample data is shown and the lines indicate mean values. **(d)** Gel-based ABPP analysis of nimbolide, JNS27, and iodoacetamide competition against IA-rhodamine labeling of recombinant human RNF114 protein. RNF114 protein was pre-treated with DMSO vehicle or nimbolide, JNS27, or iodoacetamide for 30 min prior to labeling of RNF114 with IA-rhodamine (100 nM) for 30 min. RNF114 IA-rhodamine labeling was assessed by SDS/PAGE and in-gel fluorescence. Full length and replicate blots are shown in **Supplementary Fig. 7b.** Data shown are from an n=1 biological replicates. **(e)** Pure RNF114 protein was labeled with nimbolide (100 or 1 μM, 1 h) and subjected to tryptic digestion and LC-MS/MS analysis. Shown is the nimbolide-modified adduct on C8 of RNF114. We have repeated these experiments twice. **(f)** Nimbolide-alkyne *in situ* labeling. 231MFP cells stably expressing a Flag-tagged RNF114 were treated with DMSO vehicle or nimbolide-alkyne (100 nM) for 4 h. RNF114 was subsequently enriched from harvested cell lysates and then rhodamine-azide was appended onto probe-labeled proteins by CuAAC, after which nimbolide-alkyne labeling was visualized by SDS/PAGE and in-gel fluorescence. RNF114 labeling by the nimbolide-alkyne probe were quantified by densitometry. Full length and replicate blots are shown in **Supplementary Fig. 7c.** Data shown are from n=3 biologically independent samples/group. Gels shown in **(a** and **d)** are representative gels from n=3 biologically independent samples/group. Data shown in **(b, f)** are average ± sem, n=5 for **(b)** and n=3 for **(f)** biologically independent samples/group. Statistical significance was calculated with unpaired two-tailed Student's t-tests in **(b, c, f)**. Significance is expressed in **(b)** as *p=4.52x10^{-5}, 0.0429, and 0.00230 for siRNF114-1, siRNF114-2, and siRNF114-3, respectively compared to siControl cells. Significance in **(c)** is expressed as *p=1.90x10^{-5}, 0.000272, 0.00101 for 10, 6, and 3 μM, respectively for siRNF114-1; *p=0.000626, 0.00139, 3.66x10^{-5} for 10, 6, and 3 μM, respectively for siRNF114-2; and *p=0.00134, 9.15x10^{-5}, 0.00769 for 10, 6, and 3 μM, respectively for siRNF114-3 compared to corresponding concentration of nimbolide treatment in siControl cells. Significance in **(f)** is expressed as *p=0.0188 compared to vehicle-treated controls.

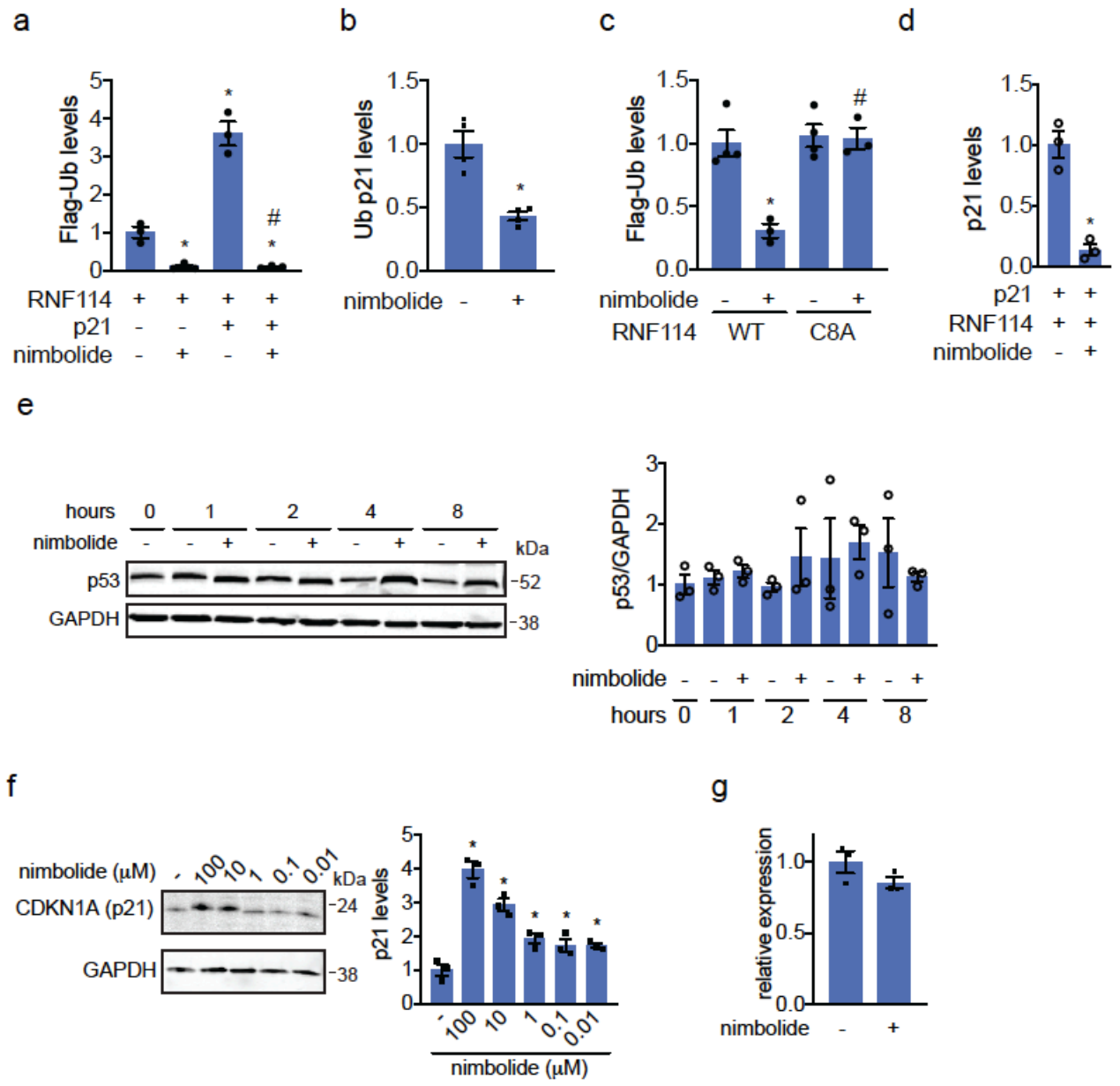

Supplementary Figure 3. Levels of p53 and p21 in nimbolide-treated 231MFP breast cancer cells. (a-d) Quantification of ubiquitinated protein blots shown in **Fig. 4a-c** and p21 levels in **Fig. 4d**, respectively. **(e)** p53 levels in 231MFP breast cancer cells treated with DMSO vehicle or nimbolide (100 μM) assessed by Western blotting alongside GAPDH as a loading control. Full length and replicate blots are shown in **Supplementary Fig. 11a. (f)** Dose-response of p21 elevation with DMSO vehicle or nimbolide treatment for 1 h, assessed by Western blotting alongside GAPDH as a loading control. Full length and replicate blots are shown in **Supplementary Fig. 7b. (g)** p21 mRNA expression levels in 231MFP cells treated with nimbolide (100 μM) for 1 h assessed by qPCR. Gels shown in **(e** and **f)** are representative of an n=3 biologically independent samples /group. Blots were quantified by densitometry and normalized to loading control. Data shown in bar graphs are average ± sem from n=3 biologically independent samples/group for **(a-g)**. Statistical significance was calculated with unpaired two-tailed Student's t-tests in **(a-g)**. Significance is expressed as *p=0.0265, 0.00461, 0.0247 for RNF114/nimbolide, RNF114/p21, and RNF114/p21/nimbolide groups compared to RNF114 DMSO vehicle treated control groups for Flag-Ub blot in **(a)**; *p=0.00201385 compared to RNF114/p21 DMSO vehicle control group for **(b)**; *p=0.00334 for WT nimbolide groups compared to WT DMSO vehicle-treated control in **(c)**; *p=0.00102 compared to the p21/RNF114 group in **(d)**; and *p=0.00518, 0.00161, 0.0145, 0.0452, 0.0187 for 100, 10, 1, 0.1, and 0.01 μM, respectively, compared to vehicle-treated controls in **(f)**. Significance expressed as #p=0.00202 compared to RNF114/p21 vehicle-treated control group in **(a)**, #p=0.0294 compared to WT nimbolide-treated group in **(c)**.

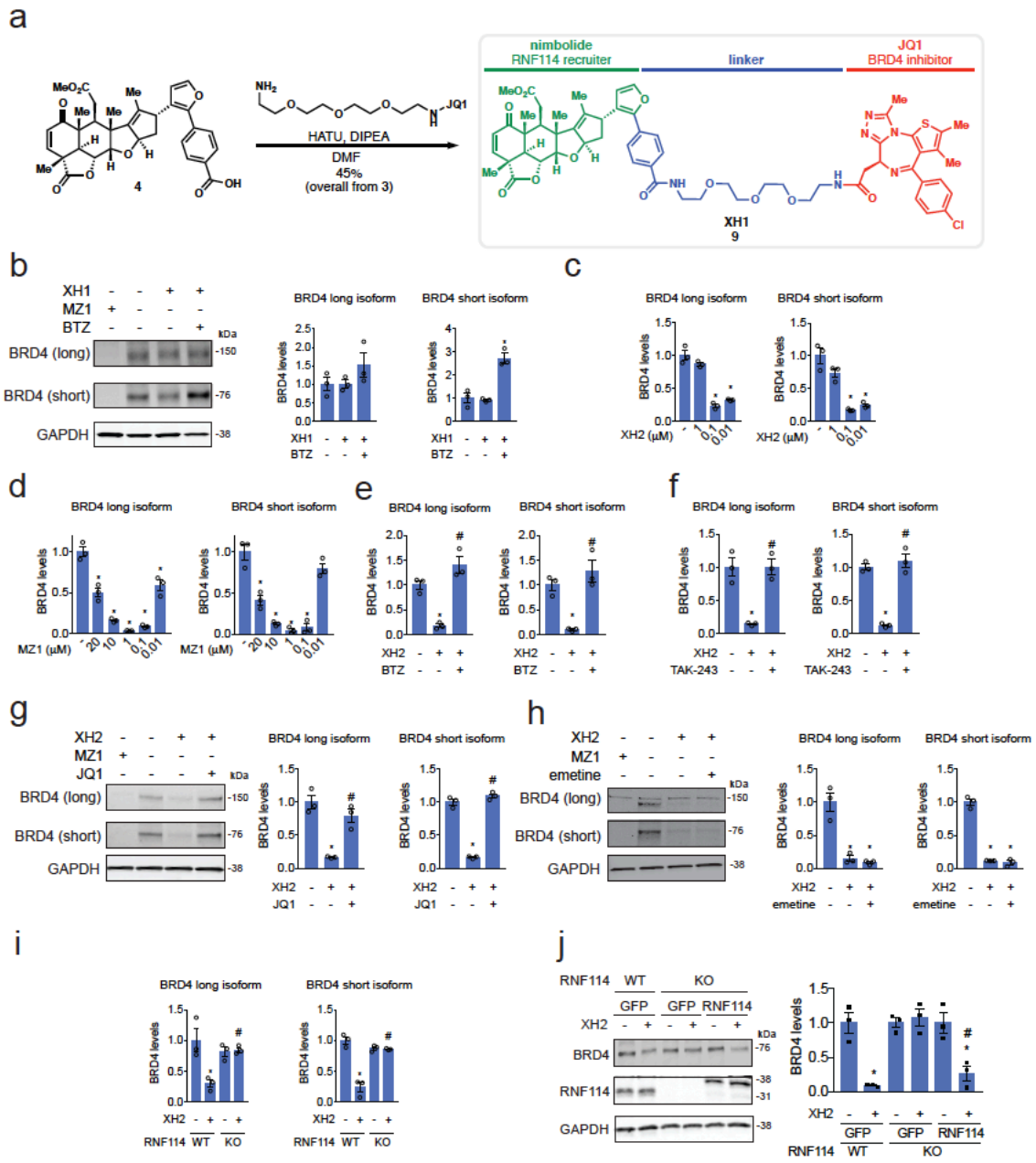

Supplementary Figure 4. Characterization of nimbolide-based degraders. (a) Synthetic route for XH1 degrader. **(b)** BRD4 levels in 231MFP breast cancer cells pre-treated with DMSO vehicle or proteasome inhibitor bortezomib (1 μM) for 30 min prior to and also during XH1 treatment (100 nM) for 12 h, assessed by Western blotting alongside GAPDH loading control. Full length and replicate blots are shown in **Supplementary Fig. 12a. (c-f)** Shown in **(c, d, e, f)** are quantification for experiments in **Fig. 5c, d, e,** and **f. (g, h)** BRD4 levels in 231MFP breast cancer cells pre-treated with DMSO vehicle, JQ1 (1 μM) **(g)**, or emetine (75 μM) **(h)** for 30 min prior to and also during XH2 treatment (100 nM) for 12 h, assessed by Western blotting alongside a GAPDH loading control. Full length and replicate blots are shown in **Supplementary Fig. 12b-12c. (i)** Quantification for experiments shown in **Fig. 5h. (j)** Effect of DMSO vehicle or XH2 (100 nM) treatment for 12 h on BRD4 expression in HAP1 RNF114 wild-type and knockout cells transiently transfected with GFP control or wild-type Flag-tagged RNF114. BRD4, RNF114, and GAPDH expression were assessed by Western blotting. Data were normalized to DMSO vehicle controls for each group. Full length and replicate blots are shown in **Supplementary Fig. 12d.** Gels shown in **(b, g, h,** and **j)** are representative images. Data shown in **(b-j)** are average ± sem from n=3 biologically independent samples/group. Statistical significance was calculated with unpaired two-tailed Student's t-tests. Significance is expressed as:

*p=0.00231 for BRD4 short isoform XH1/BTZ group compared to vehicle-treated control groups in **(b);** *p=0.000665, 0.000902 for BRD4 long isoform 0.1 and 0.01 μM, respectively, and *p=0.0019925, 0.00303 for BRD4 short isoform 0.1 and 0.01 μM, respectively, compared to vehicle-treated control groups in **(c)**; *p=0.00400, 0.000187, 9.81×10^{-5}, 0.000129, 0.01 for BRD4 long isoform for 20, 10, 1, 0.1, 0.01 μM, respectively, and *p=0.00673, 0.000902, 0.000666, 0.00104 for BRD4 short isoform for 20, 10, 1, 0.1 μM, respectively, compared to vehicle-treated control groups in **(d);** *p=0.00098186 and p=0.0169 for XH2 compared to vehicle-treated control groups for BRD4 long and short isoforms, respectively, in **(e)**; *p=0.00174, 2.55×10^{-5} for XH2-treated groups compared to vehicle treated groups for BRD4 long and short isoforms, respectively, in **(f)**; *p=0.00143, 6.23×10^{-5} for XH2-treated groups compared to vehicle treated groups for BRD4 long and short isoforms, respectively, in **(g)**; *p=0.00246, 0.00171 for XH2- and XH2/emetine-treated groups, respectively, compared to vehicle treated groups for BRD4 long isoform, and *p=3.47×10^{-5}, 5.71×10^{-5} for XH2- and XH2/emetine-treated groups, respectively, compared to vehicle treated groups for BRD4 short isoform in **(h)**; *p=0.0236, 0.00165 for WT XH2-treated groups compared to WT control groups for BRD4 long and short isoforms, respectively, in **(i);** *p=0.00344 for WT GFP/XH2 groups compared WT GFP vehicle-treated control group and *p=0.0154 for KO RNF114/XH2 groups compared to KO RNF114 vehicle-treated control groups in **(j);** #p=0.00197 and 0.00557 for XH2/BTZ groups compared to XH2-treated groups for BRD4 long and short isoforms, respectively, in **(e)**; #p=0.000817 and 0.000437 for XH2/TAK-243 groups compared to XH2-treated groups for BRD4 long and short isoforms, respectively, in **(f)**; #p=0.00389 and 1.21×10^{-5} for XH2/JQ1 groups compared to XH2-treated groups for BRD4 long and short isoforms, respectively, in **(g)**; #p=0.00166, 0.00159 for KO XH2-treated groups compared to WT XH2-treated groups for BRD4 long and short isoforms, respectively, in **(i)**; #p=0.00814 for KO RNF114/XH2-treated groups compared to KO GFP/XH2-treated groups in **(j).**

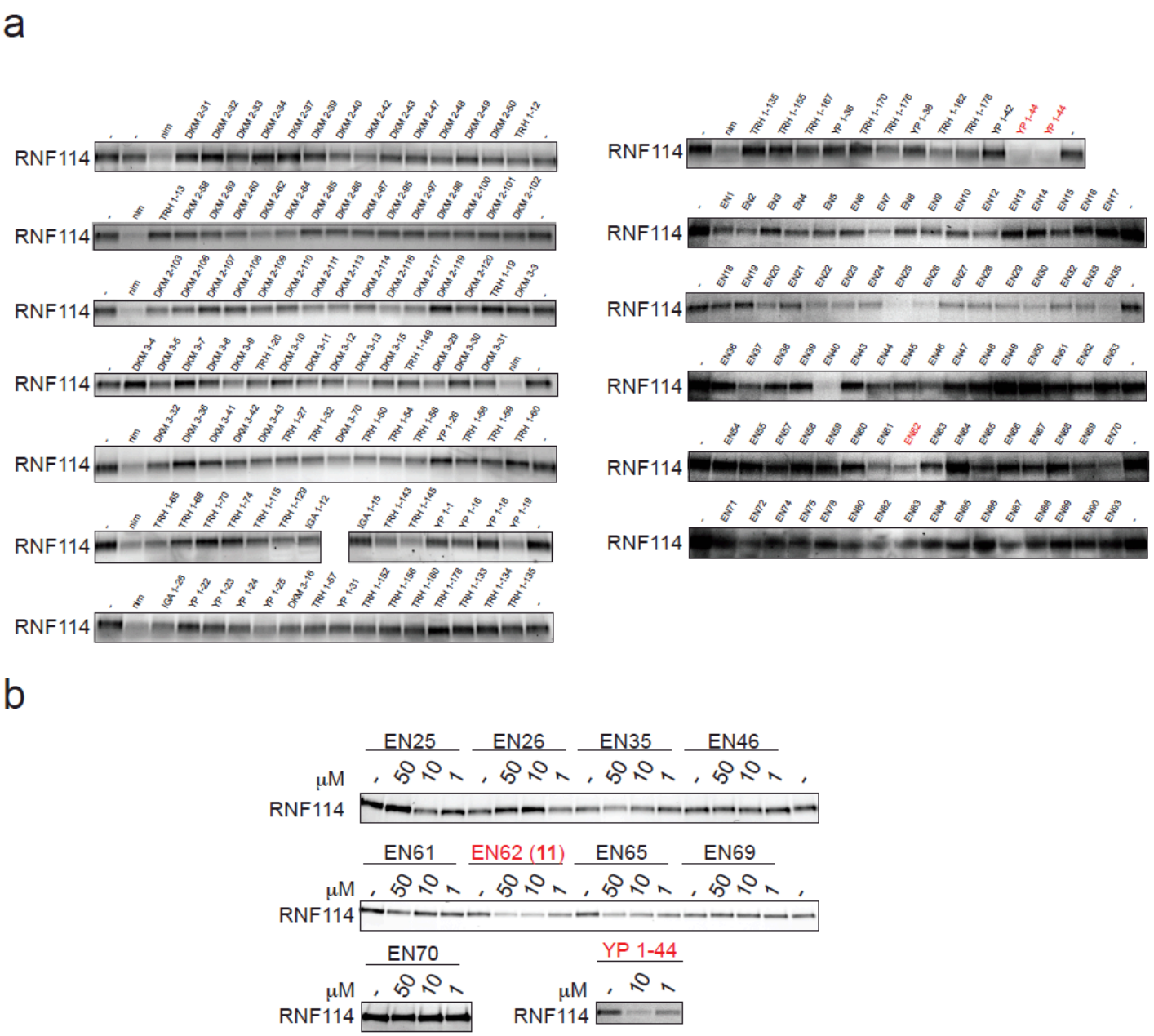

Supplementary Figure 5. Gel-based ABPP screen of cysteine-reactive ligands against RNF114. (a) Cysteine-reactive covalent ligands were screened against JNS27 labeling of pure human RNF114 protein. Covalent ligands (50 μM) were pre-incubated with RNF114 for 30 min prior to labeling with JNS27 for 1 h. Rhodamine-azide was then appended to probe-labeled proteins by CuAAC. Proteins were separated by SDS/PAGE and visualized by in-gel fluorescence. **(b)** Those proteins that showed inhibition of probe-labeling were re-tested in dose-response studies below to identify hits that reproducibly inhibited JNS27 labeling of RNF114 under the same incubation conditions described in **(a)**. Data shown in **(a)** were from n=1 biologically independent sample. Data shown in **(b)** are from n=1 biologically independent samples/group. Full length blots in **(a, b)** are shown in **Supplementary Fig. 13a, 13b.**

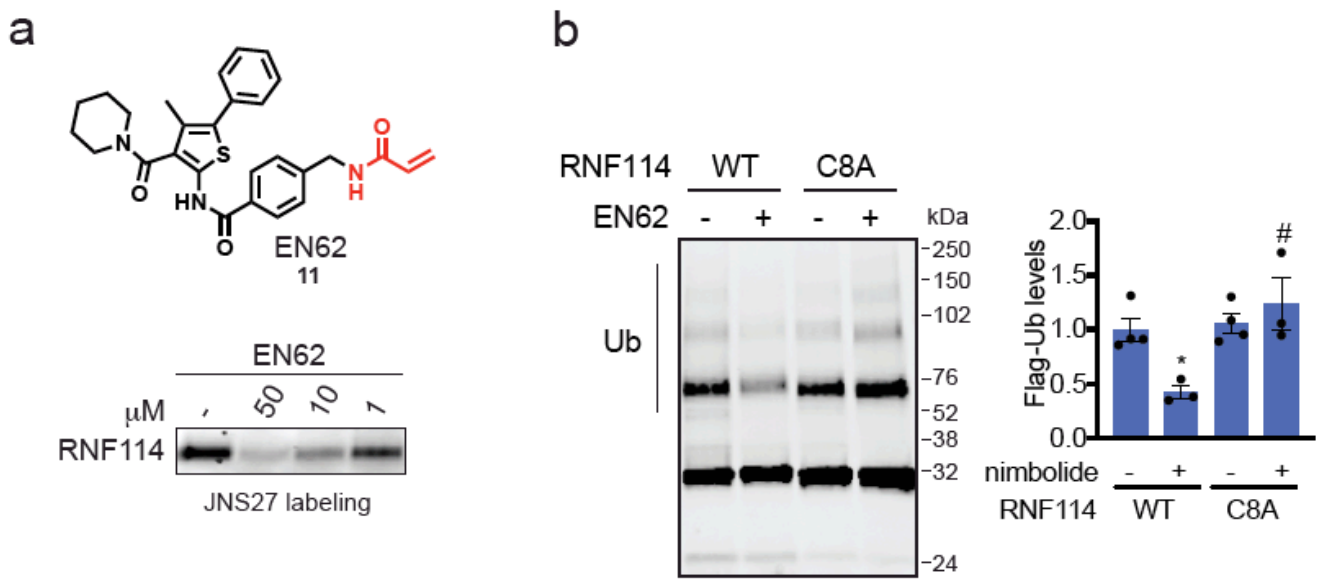

Supplementary Figure 6. Chemoproteomics-enabled covalent ligand screening to identify more synthetically tractable covalent ligands against RNF114. (a) Upon screening a library of cysteine-reactive covalent ligands against JNS27 labeling of RNF114, EN62 was one of the top hits. Shown is the structure of EN62 with the acrylamide reactive moiety highlighted in red. Shown also is a gel-based ABPP analysis of EN62 against JNS27 labeling of pure RNF114. Full length blots in **(a, b)** are shown in **Supplementary Fig. 13c. (b)** RNF114 autoubiquitination assay with DMSO or EN62 (50 μM) treatment with wild-type or C8A mutant RNF114. Gels shown in **(a-b)** are representative images from n=3 biologically independent samples/group. Data shown in **(b)** are average ± sem. Statistical significance was calculated with unpaired two-tailed Student's t-tests. Significance in **(b)** is expressed as *p=0.00787 compared to the vehicle-treated controls. Significance is expressed as #p=0.0294 compared to EN62-treated WT RNF114 protein in **(b).**

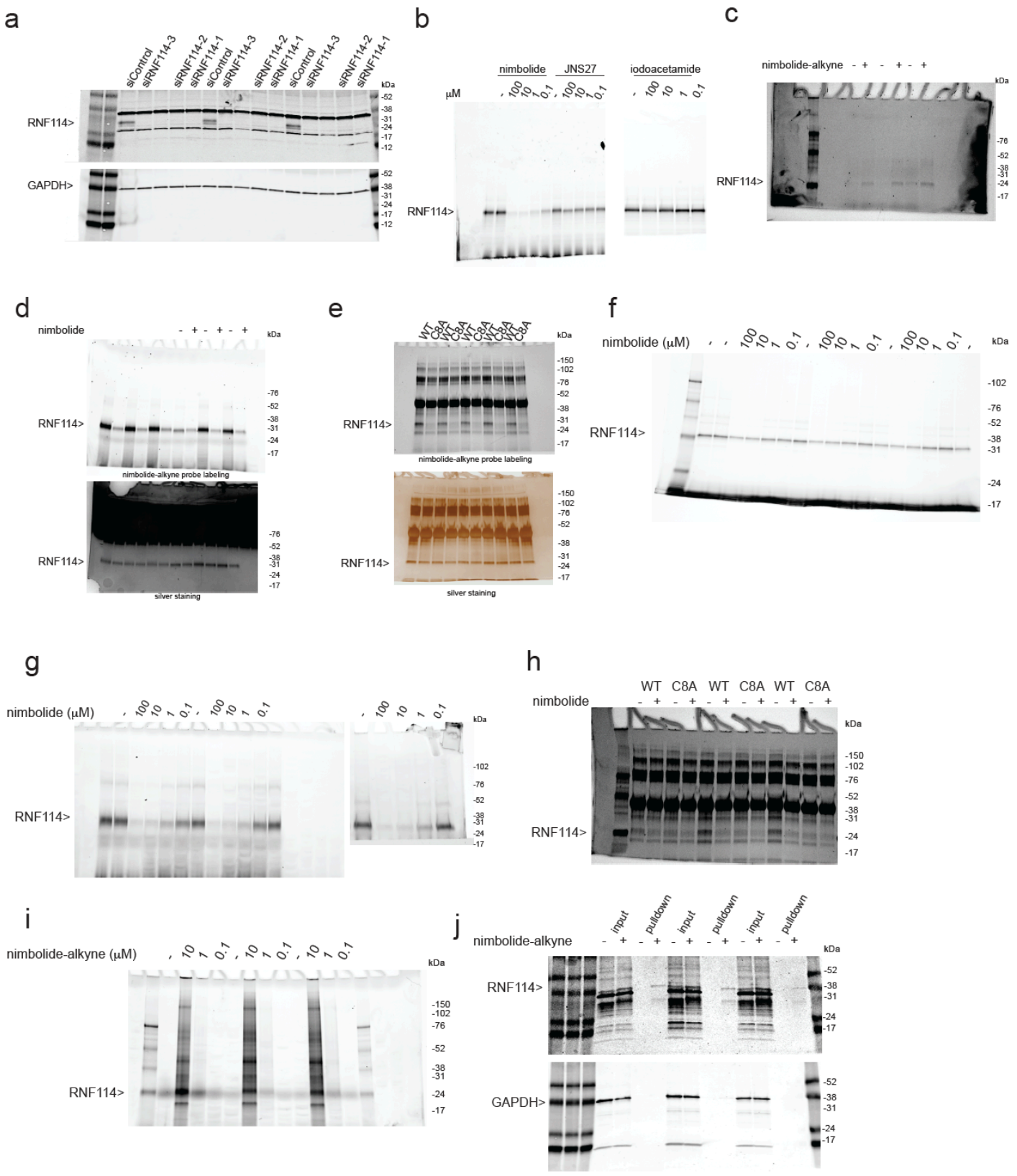

Supplementary Figure 7. Full-length images. (a) Full length and replicate blots from **Fig. 2c** and **Supplementary Fig. 2a. (b)** Full length gels from **Supplementary Fig. 2d. (c)** Full length and replicate blots from **Supplementary Fig. 2f**. **(d)** Full length and replicate blots from **Fig. 2c** top gels. **(e)** Full length and replicate blots from **Fig. 2c** bottom gels. **(f)** Full length and replicate blots from **Fig. 3d. (g)** Full length and replicate blots from **Fig. 3e** left panel. **(h)** Full length and replicate blots for **Fig. 3e** right panel. **(i)** Full length and replicate blots for **Fig. 3f**. **(j)** Full length and replicate blots for **Fig. 3g.**

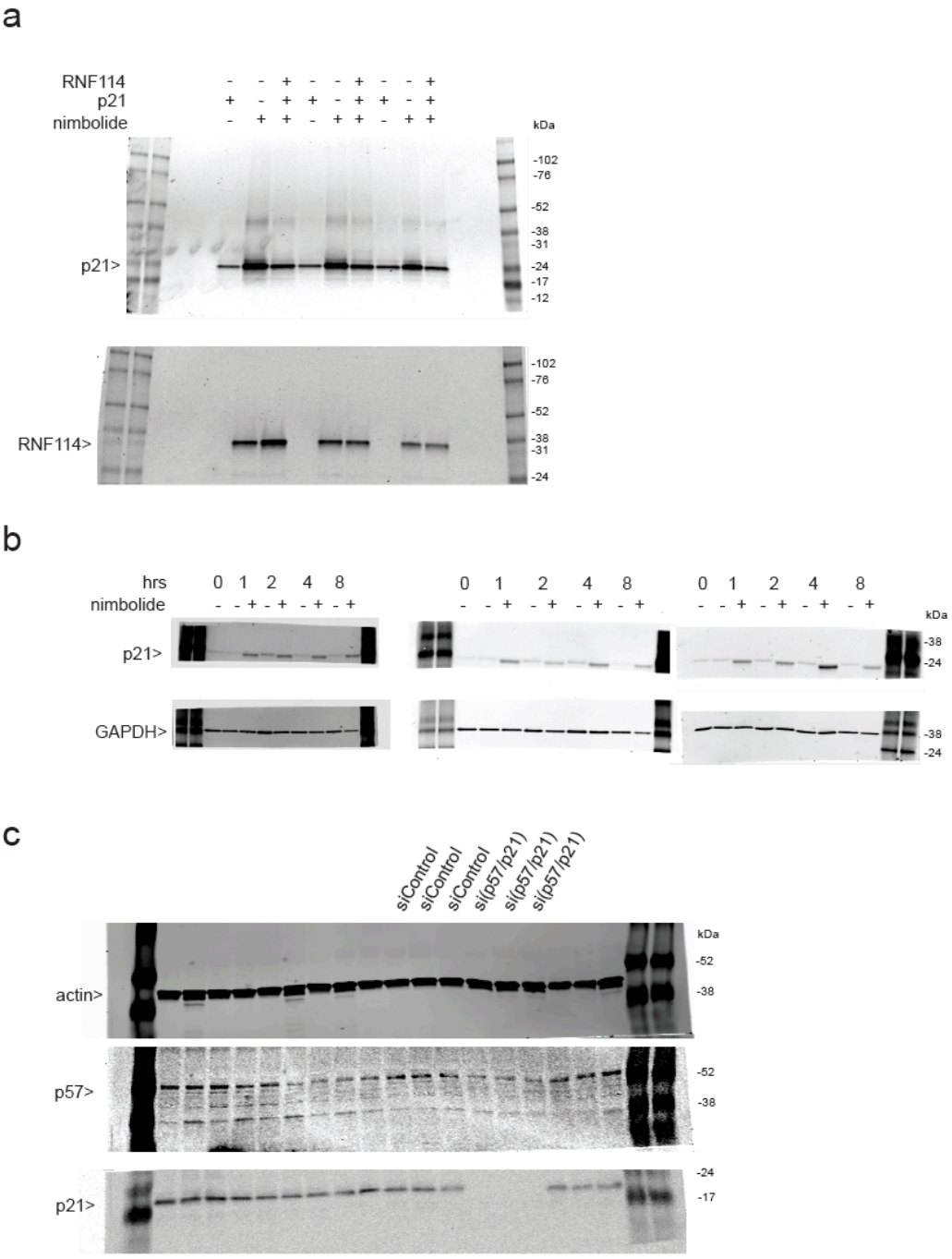

Supplementary Figure 8. Full-length images. (a) Full length and replicate blots for **Fig. 4d**. **(b)** Full length and replicate blots for **Fig. 4e**. **(c)** Full length and replicate blots for **Fig. 4h**.

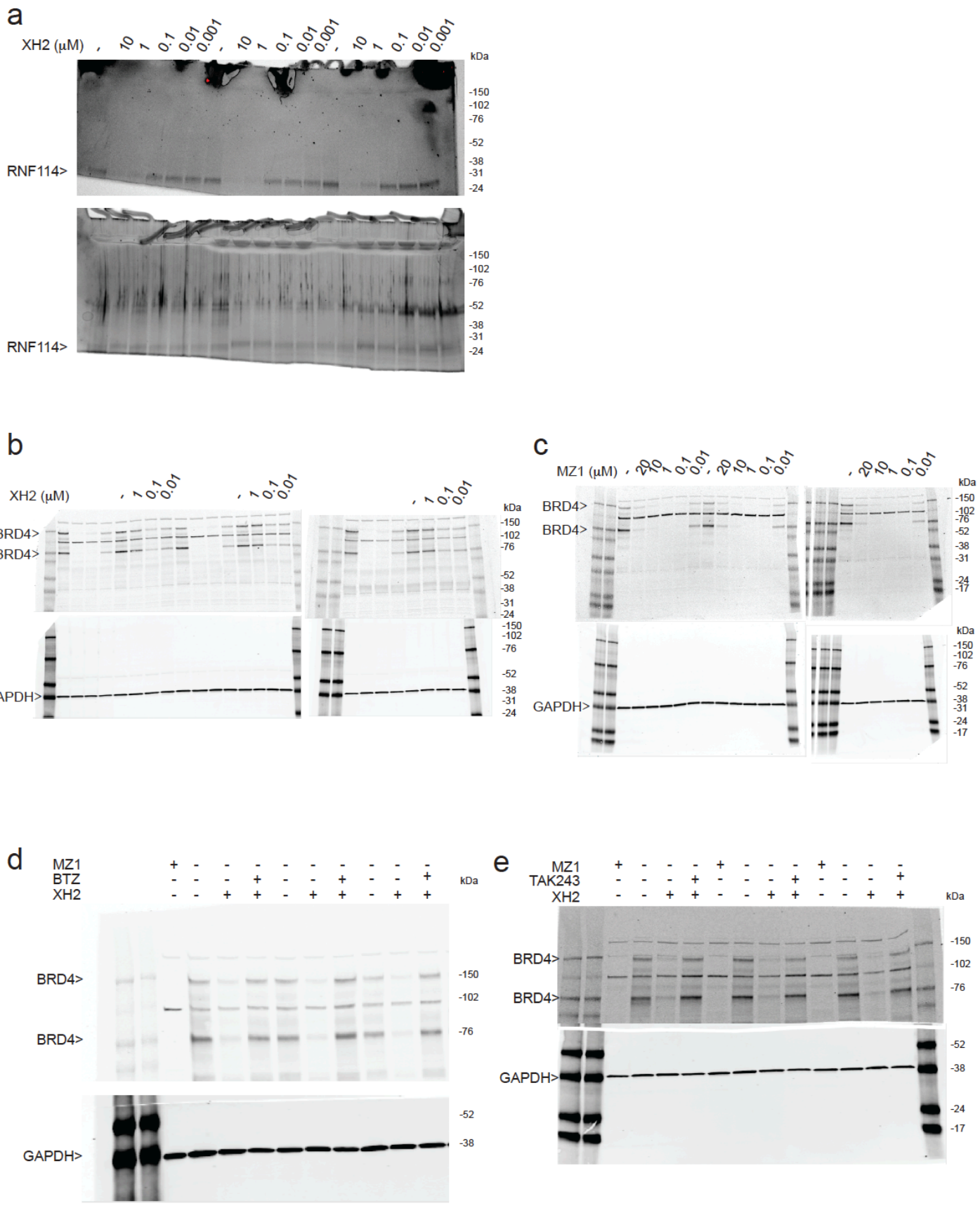

Supplementary Figure 9. Full-length images. (a) Full length and replicate blots for **Fig. 5b**. **(b)** Full length and replicate blots for **Fig. 5c. (c)** Full length and replicate blots for **Fig. 5d. (d)** Full length and replicate blots for **Fig. 5e. (e)** Full length and replicate blots for **Fig. 5f.**

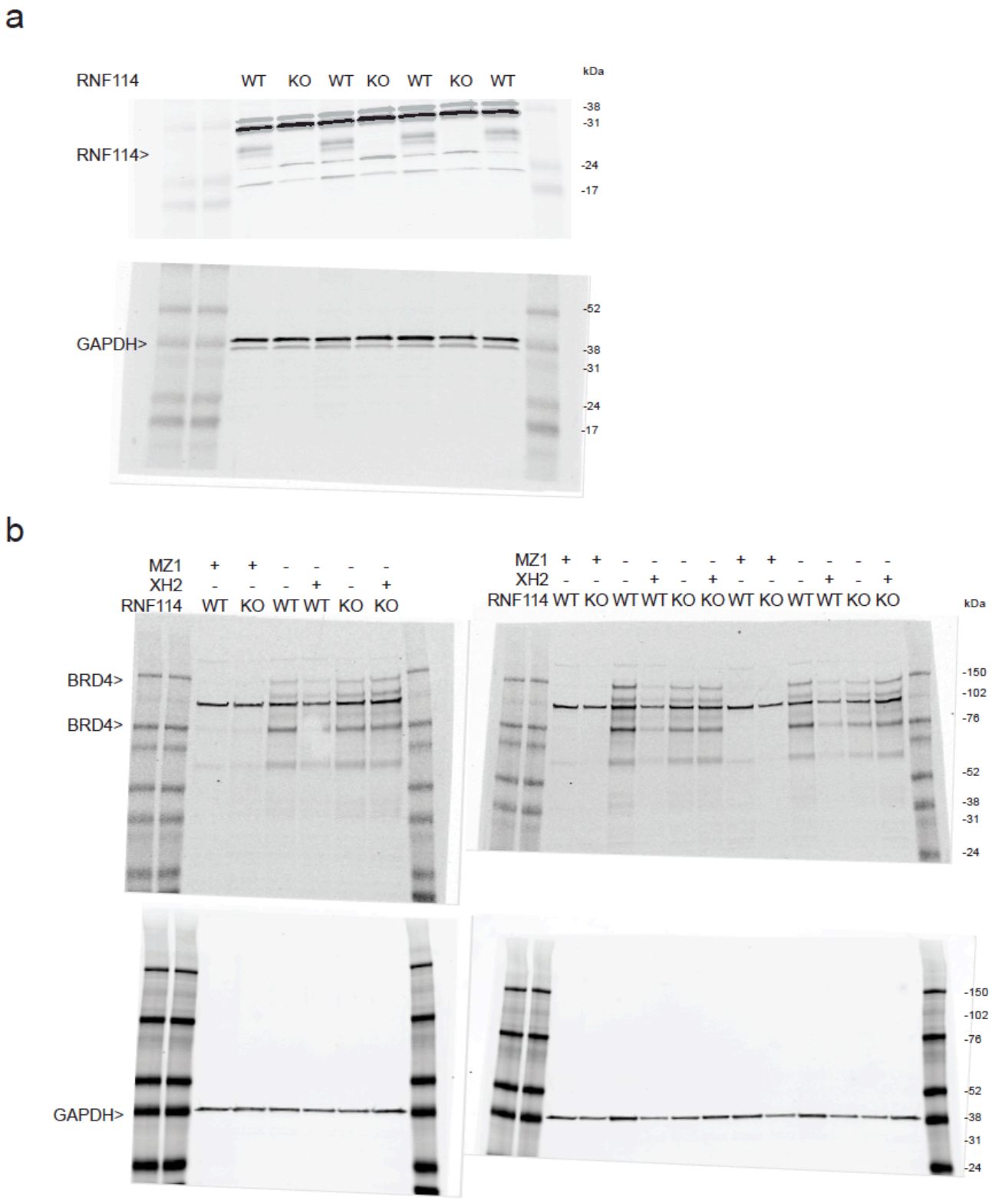

Supplementary Figure 10. Full-length images. (a) Full length and replicate blots for **Fig. 5g**. **(b)** Full length and replicate blots for **Fig. 5h.**

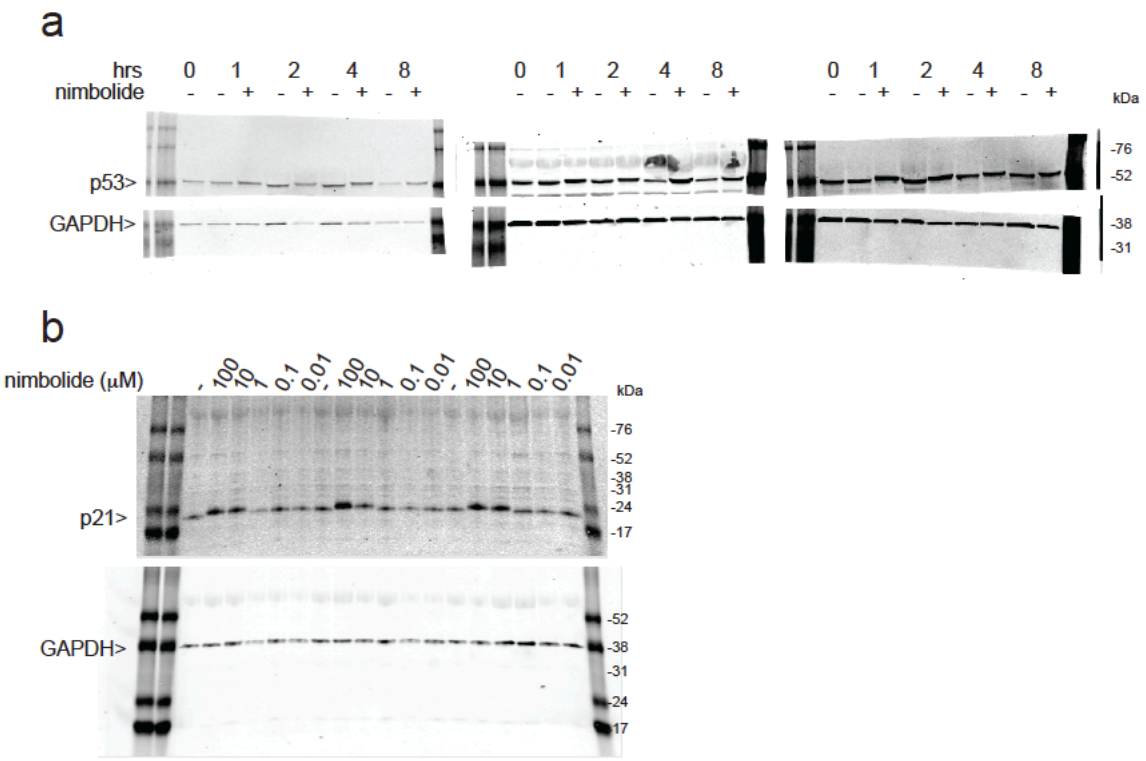

Supplementary Figure 11. (a) Full length and replicate blots for **Supplementary Fig. 3e**. **(b)** Full length and replicate blots for **Supplementary Fig. 3f**.

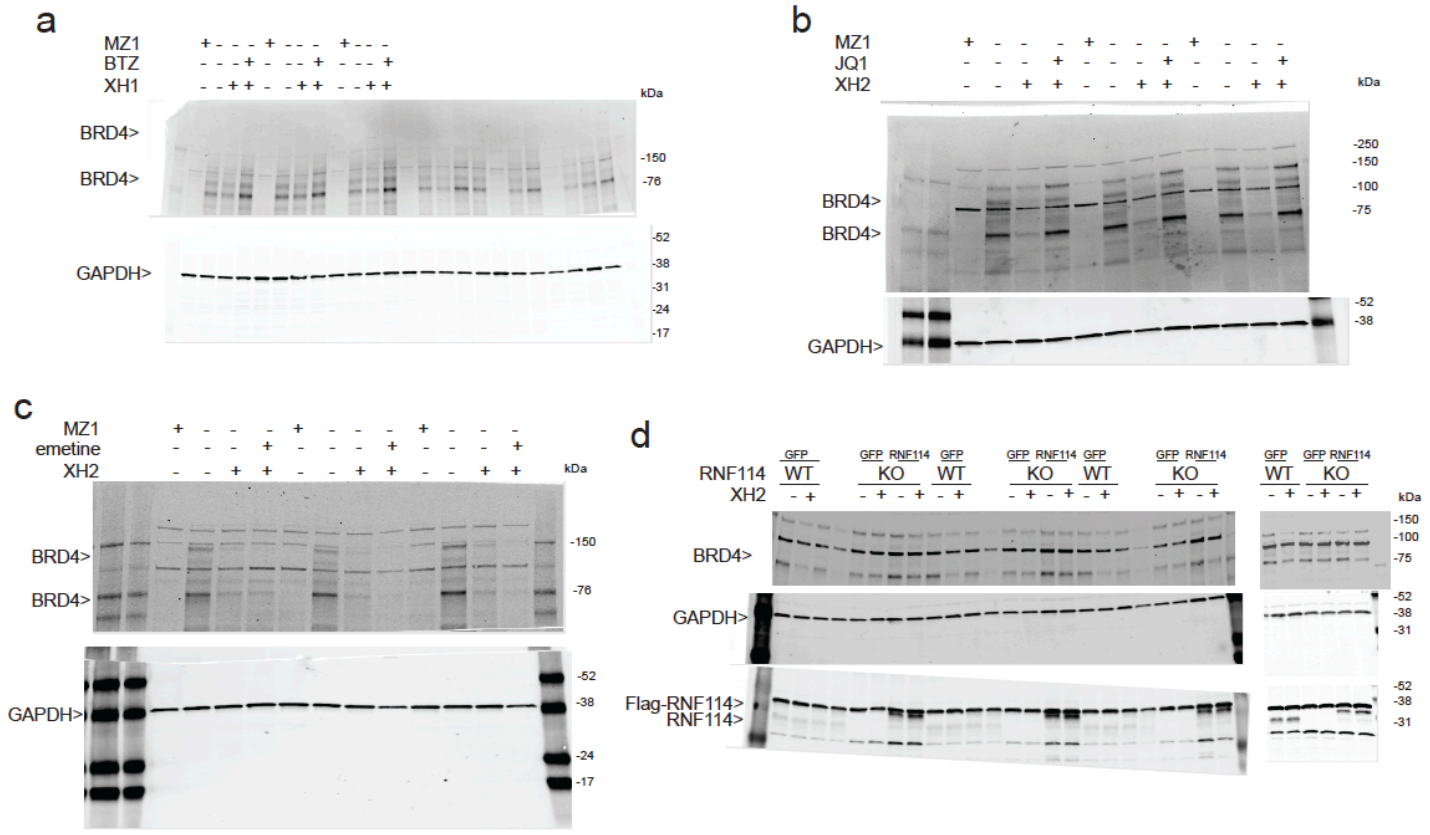

Supplementary Figure 12. Full-length images. (a) Full length and replicate blots for **Supplementary Fig. 4b**. **(b)** Full length and replicate blots for **Supplementary Fig. 4g. (c)** Full length and replicate blots for **Supplementary Fig. 4h. (d)** Full length and replicate blots for **Supplementary Fig. 4j.**

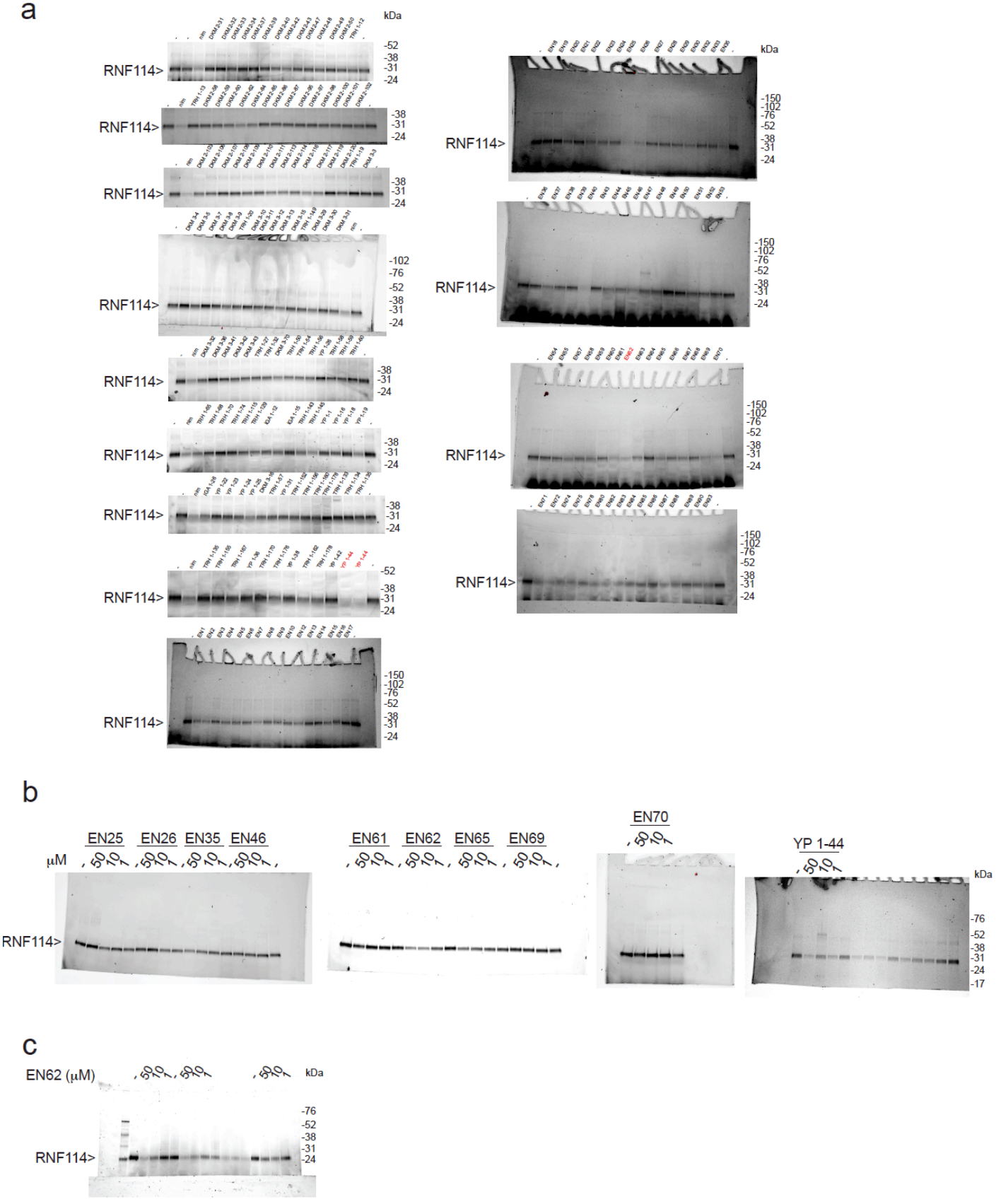

Supplementary Figure 13. Full-length images. (a) Full length blots for **Supplementary Fig. 5a**. **(b)** Full length blots for **Supplementary Fig. 5b. (c)** Full length and replicate blots for **Supplementary Fig. 6.**

Supplementary Datasets

Supplementary Dataset 1. IsoTOP-ABPP analysis of nimbolide treatment *in situ* in 231MFP breast cancer cells. IsoTOP-ABPP analysis of nimbolide treatment *in situ* (10 μM). 231MFP breast cancer cells were treated with DMSO or nimbolide (10 μM, 1.5 h *in situ*), after which cells were harvested and proteomes were labeled *ex situ* with IA-alkyne (100 μM, 1 h), followed by appendage of isotopically light (for DMSO-treated) or heavy (for nimbolide-treated) TEV protease cleavable biotin-azide tags by copper-catalyzed azide-alkyne cycloaddition (CuAAC). Control and treated proteomes were subsequently combined in a 1:1 ratio, probe-labeled proteins were avidin-enriched, digested with trypsin, and probe-modified tryptic peptides were eluted by TEV protease, analyzed by LC-MS/MS, and light to heavy probe-modified peptide ratios were quantified. Shown are data from n=3 biological replicates/group.
Tab 1. Total isoTOP-ABPP proteomic dataset
Tab 2. Analyzed isoTOP-ABPP dataset. For those probe-modified peptides that showed ratios >2, we only interpreted those targets that were present across all three biological replicates, were statistically significant, and showed good quality MS1 peak shapes across all biological replicates. Light versus heavy isotopic probe-modified peptide ratios are calculated by taking the mean of the ratios of each replicate paired light vs. heavy precursor abundance for all peptide spectral matches (PSM) associated with a peptide. The paired abundances were also used to calculate a paired sample t-test p-value in an effort to estimate constancy within paired abundances and significance in change between treatment and control. P-values were corrected using the Benjamini/Hochberg method.

Supplementary Dataset 2. TMT-based quantitative proteomic analysis of proteins enriched by nimbolide-alkyne probe *in situ* treatment in 231MFP breast cancer cells. 231MFP breast cancer cells were treated with DMSO vehicle or the nimbolide-alkyne probe (50 μM) for 1.5 h. Probe-labeled proteins were conjugated to biotin-azide by CuAAC and subsequently avidin-enriched from 231MFP proteomes and tryptic digests from enriched proteins were analyzed by TMT-based quantitative proteomics. Shown are the proteins from this experiment that showed at least 2 unique peptides, as well as TMT ratios of no-probe versus probe. The data shown are from n=3 biological replicates/group.

Supplementary Dataset 3. TMT-based quantitative proteomic profiling of XH2-treatment in 231MFP breast cancer cells. Tandem mass tag (TMT)-based quantitative proteomic profiling of 231MFP breast cancer cells treated with DMSO vehicle or nimbolide (100 nM) **(Tab 1)** or XH2 (100 nM) **(Tab 2)** for 12 h. Shown are the data for proteins identified that showed at least 2 unique peptides from n=3 biological replicates/group.

Supplementary Dataset 4. Structures of covalent ligands screened against RNF114